Author(s): Räisänen, V. I. & Alava, M. J. & Nieminen, Risto M.

Title: Failure of planar fiber networks

Year: 1997

Version: Final published version

Please cite the original version:

Räisänen, V. I. & Alava, M. J. & Nieminen, Risto M. 1997. Failure of planar fiber networks. Journal of Applied Physics. Volume 82, Issue 8. 3747-3753. ISSN 0021-8979 (printed). DOI: 10.1063/1.365737.

AIP Journal of Applied Physics

Failure of planar fiber networks

V. I. Räisänen, M. J. Alava, and R. M. Nieminen

Citation: Journal of Applied Physics **82**, 3747 (1997); doi: 10.1063/1.365737
View online: http://dx.doi.org/10.1063/1.365737
View Table of Contents: http://scitation.aip.org/content/aip/journal/jap/82/8?ver=pdfcov
Published by the AIP Publishing

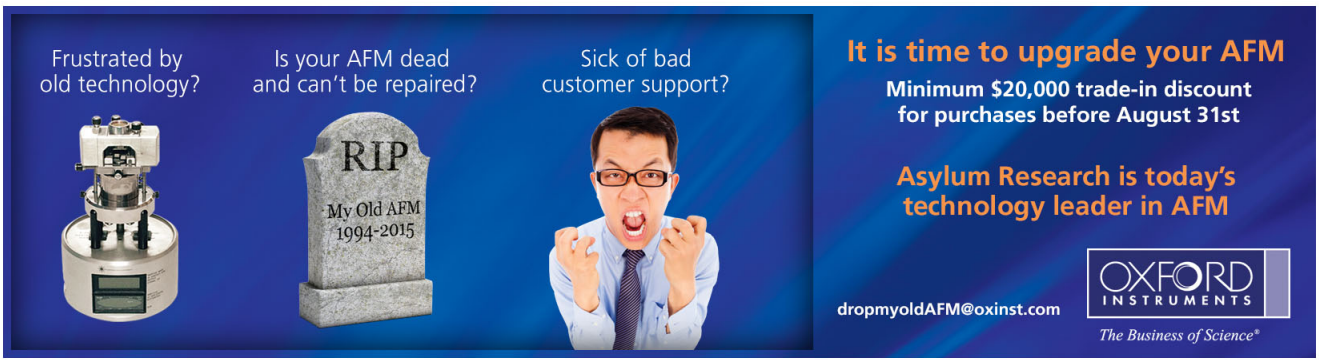

Failure of planar fiber networks

V. I. Räisänen
Centre for Scientific Computing, P. O. Box 405, FIN-02101 Espoo, Finland and ICA1, University of Stuttgart, Pfaffenwaldring 27, D-70569 Stuttgart, Germany[a)]

M. J. Alava and R. M. Nieminen
Laboratory of Physics, Helsinki University of Technology, P.O. Box 1100, HUT 02015

(Received 18 March 1997; accepted for publication 11 July 1997)

We study the failure of planar random fiber networks with computer simulations. The networks are grown by adding flexible fibers one by one on a growing deposit [K. J. Niskanen and M. J. Alava, Phys. Rev. Lett. **73**, 3475 (1994)], a process yielding realistic three dimensional network structures. The network thus obtained is mapped to an electrical analogue of the elastic problem, namely to a random fuse network with separate bond elements for the fiber-to-fiber contacts. The conductivity of the contacts (corresponding to the efficiency of stress transfer between fibers) is adjustable. We construct a simple effective medium theory for the current distribution and conductivity of the networks as a function of intra-fiber current transfer efficiency. This analysis compares favorably with the computed conductivity and with the fracture properties of fiber networks with varying fiber flexibility and network thickness. The failure characteristics are shown to obey scaling behavior, as expected of a disordered brittle material, which is explained by the high current end of the current distribution saturating in thick enough networks. For bond breaking, fracture load and strain can be estimated with the effective medium theory. For fiber breaking, we find the counter-intuitive result that failure is more likely to nucleate far from surfaces, as the stress is transmitted more effectively to the fibers in the interior. © *1997 American Institute of Physics.* [S0021-8979(97)05820-9]

I. INTRODUCTION

Random fiber networks (RFNs) form a class of materials in which disorder plays a natural role in the mechanical properties. Whether the system in question is paper, a glass fiber mat, or a randomly oriented short fiber composite, the local stresses vary widely. This phenomenon arises from fluctuations in local stress transfer,[1,2] and from local density variations. For two-dimensional (2D) fiber networks the distribution of fiber segment lengths, or parts of fibers between points of intersections between other fibers, is essentially exponential.[3] The distribution of axial stresses in 2D networks is exponential even at high densities, and the decay parameter of the distribution turns out to be independent of density.[4] Very little is known about three-dimensional random fiber networks or short fiber composites in terms of how the disorder affects elastic properties and how it correlates with local variations in structure.

In the post-elastic regime, the existing knowledge is even sparser regardless of whether the micromechanical response of the fibers and/or the network is assumed to be brittle, plasticity dominated or even viscoelastic. For 2D RFNs the local development of yield events (assuming fibers that yield) is less correlated in the direction perpendicular to external strain than in lattice models.[5,6] Fracture in 2D RFNs seems to depend qualitatively on whether one allows the breakdown of fibers or fiber-to-fiber bonds.[7] The extension of such studies[4,5,8,9] to 3D structures would seem to be prohibitively heavy computationally, because of detail and also due to the limitations of the (commercial) Finite Element Method packages commonly used.

In this paper we present a lattice model for a planar, layered fiber network. The structure is mapped to a brittle random fuse network, a scalar lattice model, in order to achieve numerical efficiency.[10] Because of the ''layered'' geometry[11] in the model, the third dimension corresponds effectively to an adjustable connectivity between fibers in a 2D model. In other words either two fibers, one on the top of the second, are in contact or there is a pore in between. Our model is thus designed to emulate the effect of the 3D network geometry on the elastic and strength properties of planar fiber networks.

What is then known—theoretically—about the structure the networks studied here? At high enough coverages, the structure becomes statistically homogeneous in the out-of-plane direction. For very low coverages there are of course no pores and the geometry is described exactly by the 2D limit. In the asymptotic limit the distributions for both pore height and diameter are exponential,[12] as one would also expect for 2D networks for large pores.[3] These local inhomogeneities are expected to lead to local stress/current fluctuations. The role of the finite thickness of the system will thus also depend on how the statistics of the fluctuations change with coverage.

The computational model used is defined in Sec. II. The electrical equivalent of the distribution of stresses as well as that of elastic modulus in the system is derived in Sec. III by using an effective medium -type argument. In Sec. IV we discuss the effect of the relative breaking limits of fibers and bonds on the fracture properties. The numerical results are presented in Sec. V, and we finish our paper with a discussion of the results in Sec. VI.

[a)]Current address of author.

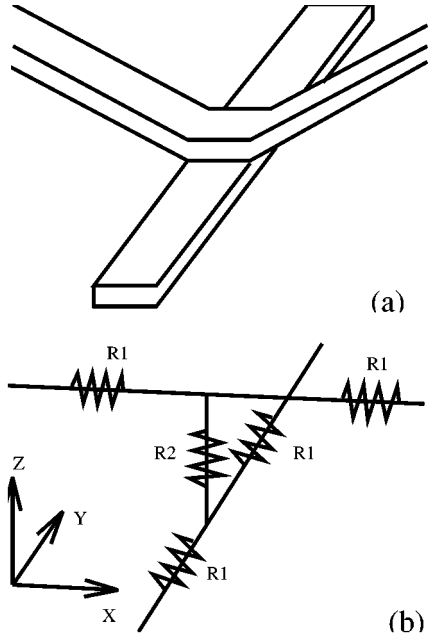

FIG. 1. A schematic representation of a detail of the connectivity in the simulation lattice. The mechanical contact, resulting from bending of a fiber out of plane (a) is mapped into a bond $R2$ between layers in the electric model (b).

II. COMPUTATIONAL MODEL

The fiber networks used are created as follows.[11] We take a fiber to be a beamlike object with finite width and thickness. Such fibers are deposited one by one on a xy-oriented substrate with square lattice geometry. The length and width of the fibers are discretized to integer values. The location and direction of each fiber (either along the x or the y axis) are chosen randomly.

When a fiber is added to the structure, it is put on the top of the network below it. If we would be interested in infinitely flexible fibers there would be no pores in between the new fiber and the old ones. To get a 3D porous network structure a bending constraint is used. The maximum z-directional displacement a fiber can make between two neighboring lattice points is limited to be at most T_f, which is thus a flexibility parameter. In other words the steps that the fibers make in the z direction are of finite height, smaller or equal to T_f. A larger value of T_f corresponds simply to more contacts with underlying fibers. T_f is measured most conveniently in units of fiber thickness t_f in the z direction, and thus one can for instance limit the undulation of a fiber to be at most 0.5 fiber thicknesses over one lattice spacing in the xy direction ($T_f = 0.5$). This gives rise to pores in the z direction, since a fiber may not be able to bend downwards enough to touch the one below it. The limit of truly 2D network is reached when $T_f \to \infty$.

The structure of the fiber network from the deposition model is mapped to a *topologically equivalent* network in a cubic lattice. By topological equivalence we mean that the fibers are connected in the same way in both models. In the cubic lattice model, the fibers are straight and are located in xy layers. z-directional connections between fibers in different layers are formed if the corresponding fibers in the fiber network from the growth model are in contact (Fig. 1). Note that we do not scale the conductivity of the fuses making up $R2$ in the figure to keep the total conductivity constant. Also, the conductivity of the fibers in our simple model is the same regardless of how the fiber undulates in the structure or is bent.

In the rest of the paper, we refer to the parts of fibers between two adjacent connections with other fibers as *segments*. The connections between fibers in different layers are called *bonds*. Conductivity inside one layer (in a fiber) is defined using σ_{xy}, and between layers (connection between two overlapping fibers) it is $\sigma_z = 5 \times \sigma_{xy}$ unless noted otherwise. This corresponds to easy current flow between layers. The connection between two lattice points breaks when the current flowing through it exceeds a predefined threshold. This threshold for fiber segments is i_c^{xy} and for bonds $i_c^z = 100 i_c^{xy}$ except for part of the results in Sec. IV.

External voltage is applied in the x direction, and free boundary conditions are imposed in the y and z directions. The equilibrium distribution of currents is obtained with the Conjugate Gradient method. The connection between lattice points with the largest current is removed, after which the equilibrium state is recalculated. This procedure is continued until the point is reached in which no current is passing through the lattice. Systems with sizes $20 \times 20 \times N_f$, $50 \times 50 \times N_f$, and $80 \times 80 \times N_f$ have been used. N_f has been chosen to correspond to 1.25–6.25 times the geometrical percolation density $N_{f,c}$ of the system. For the flexibility parameter we have used the values $T_f = 0.25$, 0.5, 1, 2 and 4. The last value, $T_f = 4$, is already a good approximation of the limit of infinitely flexible fibers.[11] Finally, the value $l_f = 7$ lattice spacings was used for the length of the fiber. Note that the model as defined above is a standard random fuse network one, the only differences being that the local geometry is now obtained from a ''real'' microstructure and that intralayer connections have different breaking and conductivity properties from the in-plane ones.

In what follows one should take note of the correspondences between electrical and elastical quantities. The RFN simulations mimic elongative tensile tests with $I \leftrightarrow F$ (current corresponds to force), $V \leftrightarrow \Delta x$ (applied voltage corresponds to imposed elongation) and $\Sigma \leftrightarrow E$ (conductivity corresponds to elastic modulus). For the fuse elements one can map the local current to axial stress (shear stress for intra-fiber bonds) and the local voltage to strain.

III. CURRENT DISTRIBUTION AND EFFECTIVE CONDUCTIVITY

Next we use an effective medium approximation (EMA)-type argument to derive the distribution of currents in the system and to discuss the scaling of conductivity with the stress/current transfer (the σ_z to σ_{xy} ratio). In other words, the segments in a fiber are thought to be independent of each other and to be embedded in an average background. Let us assume that the distribution of segment lengths l_s is exponential, or

$$n(l_s) = C e^{-\alpha l_s}. \tag{1}$$

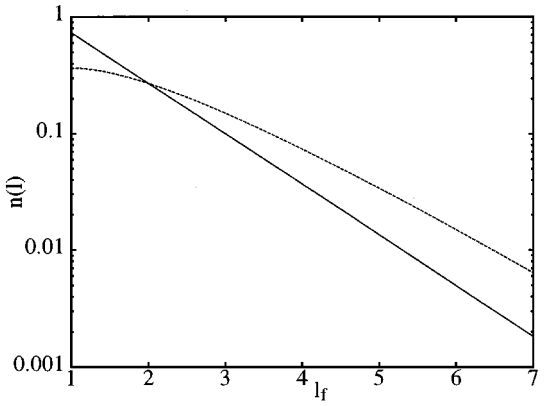

FIG. 2. The relative frequencies of bond (solid line) and segment (dashed line) type fuses plotted against the length of the segment they are parts of. In the data shown, $\alpha=1$.

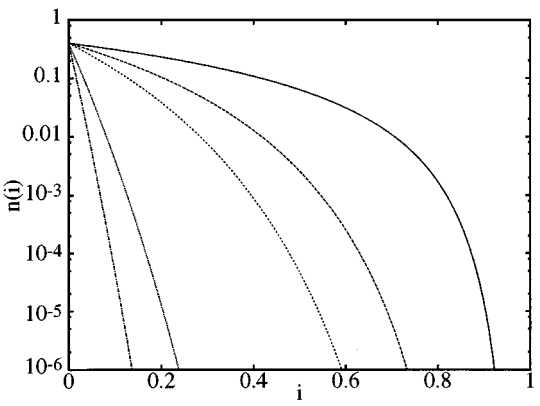

FIG. 3. Current distribution (both bond and segment fuses) obtained using the effective medium argument. From top to bottom: $\alpha=1$, 5, 10, 50, and 100. $\sigma_s/\sigma_b=2/5$.

Above, C is a normalization constant and α is the decay parameter of the distribution. The assumption of an exponential form for the segment length distribution is true for 2D random fiber networks[4] and should also hold[12] for the 3D case of the deposition model.[11] Each fiber segment is assumed to consist of l_s ''segment''-type fuses, each with conductivity σ_s. In Fig. 2 the relative frequency distributions of ''segment'' fuses and ''bond'' fuses belonging to a segment of length l_s are shown versus the segment length.

The fiber segment is supposed to be attached to a homogeneous background with two ''bond''-type fuses with conductivity σ_b. The total conductivity σ_f of the fiber segment is then

$$\sigma_f=\frac{\sigma_b\sigma_s}{l_s\sigma_b+2\sigma_s}. \tag{2}$$

The current in the sequence consisting of a fiber segment and two bonds can be expected to be proportional to its conductivity per length unit, i.e.,

$$\frac{\sigma_f}{\sigma_s l_s}=\frac{1}{1+(2/l_s)(\sigma_s/\sigma_b)}\propto i. \tag{3}$$

The current distribution $n(i)$ can be solved from Eqs. (1) and (3) by making a change of variable in the distribution:

$$n(i)=n(l_s)\frac{\partial i}{\partial l_s}. \tag{4}$$

Taking into account that there are l_s ''segment'' fuses and two ''bond'' fuses for each segment, we finally get

$$n(i)=C\frac{\sigma_s}{\sigma_b}(1-i)^2\left(1+\frac{\sigma_s}{\sigma_b}\frac{i}{1-i}\right)\exp\left(-2\alpha\frac{\sigma_s}{\sigma_b}\frac{i}{1-i}\right). \tag{5}$$

Above, current per bond has been expressed in the units of current flowing through a fuse with conductivity σ_s.

The calculation gives an exponential decay for the current distribution for relatively large values of α (Fig. 3). In the 2D limit, α is inversely proportional to density of fibers per unit area.[3] In the limit in which the fiber network structure becomes statistically invariant—except for the upper and lower surfaces—α is related to the pore number,[11,12] i.e., the probability that a fiber is not in contact with the one below or above it. However, the dependence is nontrivial in the interesting regime $T_f\sim 1$. To give the reader an idea, the average coordination number or the probability that a fuse belonging to a fiber segment is connected to another segment's is $P_c\approx 0.5$ for $T_f=1$ and $P_c\approx 0.16$ for $T_f=0.25$. Also, the local Poissonian density fluctuations are expected to create rare configurations that contribute to the high-current end of the current distribution, but not to the global conductivity.[13]

Using our result for the conductivity per length unit of a fiber, Eq. (3), a Kirkpatrick-type calculation[14] can be made to obtain the effective conductivity σ_{eff} of a lattice consisting of segment and bond fuses. The essential part of the calculation is to derive an equation for the conductivity of a lattice using the knowledge that the average value of voltage fluctuations (with respect to the average value of voltage in the system) is zero. This leads to the equation

$$0=\left\langle\frac{\sigma_{eff}-\sigma}{\sigma_{eff}+\sigma}\right\rangle, \tag{6}$$

where the effective conductivity of the background has been denoted with σ_{eff} and the fluctuating local conductivity with σ.

In our case the current distribution, Eq. (5), is equal to the distribution of conductivities whereby Eq. (6) is equivalent to the integral

$$0=\int_a^b n(i)\frac{\sigma_{eff}-i}{\sigma_{eff}+i}di, \tag{7}$$

from which σ_{eff} can, in principle, be solved. Above, the integration limits a and b for current are obtained from Eq. (3) by inserting alternatively $l_s=1$ (minimum segment length, i.e., the lattice constant) and $l_s=l_f$ (fiber length). We have calculated a few numerical approximations for the solution of Eq. (7), corresponding to the average conductivity per unit area in the limit in which the thickness of the fiber network is large. These are given in Fig. 4. As an example, let us consider the case that we have made the numerical simulations with $\sigma_s/\sigma_b=0.2$. For this particular ratio of con-

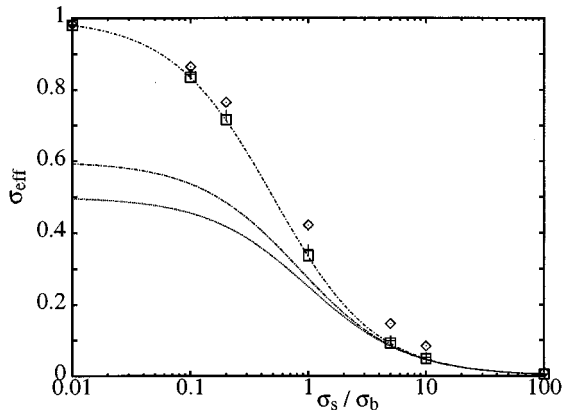

FIG. 4. Effective conductivity (σ_{eff}) as obtained from the effective medium calculation [Eq. (7)]. ($\diamond$) $\alpha=1$, (+) $\alpha=10$, ($\square$) $\alpha=100$; lines from top to bottom: $\alpha=100$, 1.5 and 1 for the prediction which is obtained by using the mean value of fiber length in Eq. (3) instead of the full distribution [Eq. (1)].

ductivities, $\sigma_{eff}\approx 0.72-0.79\times\sigma_s$ for $\alpha=1-100$. We also plot the development of $\sigma_{eff}(\sigma_s/\sigma_b)$ which is obtained by using the mean segment length instead of the true $P(l_s)$ distribution. As can be expected, the results differ quite a bit from the ''full'' l_f data for small values of α (i.e., broad segment length distribution). For a more steep segment length distribution the ''averaged'' data agree very well with the results obtained with $P(l_f)$. This is just an indication that the average segment length is approximately equal to unity.

If the distribution of conductivities decays quickly, σ_s/σ_b has a stronger effect on the total conductivity σ_{tot} since there are more short segments where σ_b is relatively more important. If one looks at the effect of the decay parameter as a function of σ_s/σ_b, it is clearly seen that the larger the conductivity of the ''bond'' fuses is, the less α affects σ_{tot}. At the limit $\sigma_b\to\infty$, $\sigma_{tot}\to 1$ in units of σ_s and at the limit $\sigma_b\to 0$, $\sigma_{tot}\to 0$ as can be expected. In the former case the currents are the same for all segments independent of l_s and in the latter case all current goes through the longest ($l_s=l_f$) segments.

IV. THE EFFECT OF BREAKING LIMITS AND THE EFFECTIVENESS OF INTER-LAYER CURRENT TRANSFER

Next we test the consequences of the ratio of the breaking limits of bonds and fiber segments, $r_1=i_c^z/i_c^{xy}$, and the ratio of the intra-layer conductivity to that inside the layers, $r_2=\sigma_z/\sigma_{xy}$. In the case of the elastic problem, corresponding quantities would be the ratios of the breaking stresses (r_1) and of elastic moduli (r_2).

Depending on the values chosen for r_1 and r_2, one would expect two general, different scenarios: if the bonds are weak (small r_1), much delocalized damage is expected.[15] This is similar to the accumulation of matrix damage in short fiber composites, when the fibers are less prone to failure than the matrix. On the other hand, if the fibers are weak (large r_1), the failure of the network should be governed by ''rare event''-type statistics, i.e., the strongest current concentration that the network geometry produces sets the fracture point.[16] In between these two extremes, when both the fibers and ''the matrix'' are weak, one expects to see crossover behavior.

To characterize the failure process, we have studied whether the broken connections are aligned in the z direction (a bond) or inside the xy plane (part of a fiber). These were designated with N_b^z and N_b^{xy}, respectively. The total number of broken connections is then $N_b=N_b^z+N_b^{xy}$. We also compare the macroscopic failure current I_b (force in the elastic case) and voltage V_b (displacement), and vary the bond quantities i_c^z and σ_z to have comparable results. A system size of 4.5 fiber lengths in linear dimension ($4.5\times l_f$ lattice spacings) and an areal density of fibers that is 3.75 times the 2D percolation coverage are used. The value of the flexibility parameter T_f is one here.

The results show that once $r_1>2$ (i.e., the breaking limit of fiber segments is at least two times lower than that of bonds), r_1 has no further effect on any of V_b, I_b or N_b. Thus data with $r_1>2$ is not included. In fact, if $r_1>1$, neither r_1 nor r_2 has a significant effect on N_b or I_b (Table I). Naturally, the breaking potential V_b increases with decreasing conductivity between layers independent of r_1. As can be expected, only bonds break if $r_1<0.5$, whereas if $r_1>1$ only fibers do so. If $i_c^z=i_c^{xy}$, fracture takes place mostly in fiber segments because the external current is flowing in the x direction. The weak bond result shows that one cannot increase the toughness of a fiber network by inhibiting fiber failure with weak matrix/contacts.

Large fluctuations show up in the breaking potential when the conductivity between layers is small ($r_2=0.1$). Physically, this means that the system is brought closer to the percolation threshold due to increasing isolation of layers. The scaling of the breaking potential is approximately $V_b\sim r_2^{-0.3}$. When bonds are weaker than fiber segments ($r_1<1$), N_b increases and both V_b and I_b decrease with de-

TABLE I. Scaling of V_b, I_b, N_b^{xy} and N_b^z as functions of r_1 and r_2. System size is 4.5×4.5 fiber lengths, $T_f=1$ and $N_f=3N_{f,c}$.

	V_b				I_b				N_b^{xy}/N_b^z			
$r_2\backslash r_1$	0.1	0.5	1.0	2.0	0.1	0.5	1.0	2.0	0.1	0.5	1.0	2.0
0.1	10.4±1.2	48.6±6.1	80 ±28	75 ±19	1.5±0.6	6.6±0.8	9.4±1.5	9.2±1.1	0/41±6	2±2/32±5	26±4/7±4	34±4/0
0.5	4.4±0.4	22.0±2.0	30.4± 1.0	31.0± 1.9	1.5±0.2	7.6±0.8	11.0±1.6	10.6±1.9	0/42±7	2±2/33±4	19±4/6±2	31±6/0
1.0	3.5±0.4	17.7±1.9	23.4± 0.2	24.4± 1.5	1.6±0.2	8.1±1.0	10.8±1.3	10.9±1.4	0/39±2	1±1/33±4	24±1/4±2	28±6/0
2.0	3.0±0.3	15.2±1.7	19.6± 1.7	20.5± 2.3	1.6±0.2	8.2±0.8	11.3±0.3	11.5±1.2	0/41±4	2±1/35±6	19±4/5±3	28±7/0
4.0	2.6±0.2	13.2±1.0	17.0± 0.7	18.0± 2.3	1.6±0.2	8.2±1.0	11.3±1.0	11.7±1.6	0/46±9	2±1/37±9	21±6/4±3	25±5/0

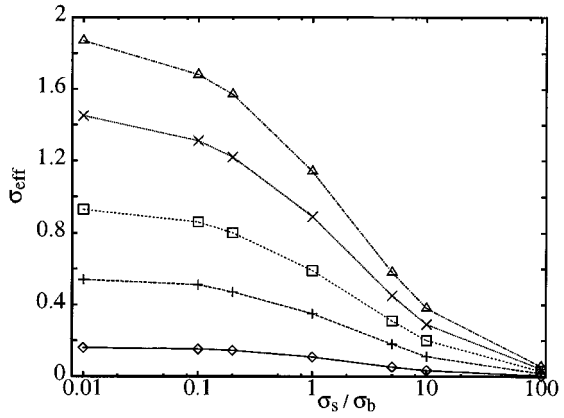

FIG. 5. Effective conductivity of the lattice obtained from numerical data. $T_f=1$, system size$=7l_f\times 7l_f$. (△) $N_f=6.25N_{f,c}$, (X) $N_f=5N_{f,c}$, (□) $N_f=3.75N_{f,c}$, (+) $N_f=2.5N_{f,c}$, (◇) $N_f=1.25N_{f,c}$. In comparing the simulation results to Fig. 4, please note that here conductivity grows with N_f. In Fig. 4 the maximum conductivity is always equal to unity.

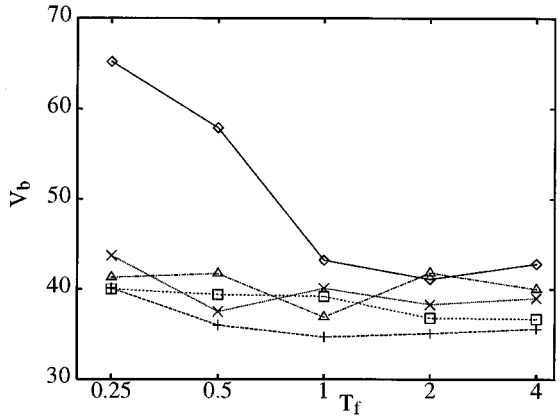

FIG. 6. Breaking potential as a function of fiber flexibility for $N_f=1-5\times N_{f,c}$ for a system of size $11l_f\times 11l_f$ in the xy plane. (△) $N_f=6.25N_{f,c}$, (X) $N_f=5N_{f,c}$, (□) $N_f=3.75N_{f,c}$, (+) $N_f=2.5N_{f,c}$, (◇) $N_f=1.25N_{f,c}$.

creasing r_1. The scaling of the fracture quantities as a function of r_1 is approximately $N_b\sim e^{r_1/1.7}$ and both V_b and $I_b\sim\ln(r_1)$. Except for the case of V_b, r_2 has no effect on fracture characteristics when $r_1<1$. The total number of broken connections saturates to a constant value at $i_c^z\approx i_c^{xy}$. Both the breaking potential and the breaking current are linearly decreasing functions of r_1 when $r_1<1$. The values $r_1=100$ and $r_2=5$ used by us in the subsequent simulations have been chosen to be in the ''safe'' region, where well-defined pure fiber-breaking behavior is seen.

Interestingly, both V_b and I_b change linearly as a function of r_1 when $r_1<1$. This suggests that in this regime (breaking takes place mostly in bonds) EMA -type argumentation may be used to obtain predictions for fracture load. It is understandable that the effective medium argument works better in the case of bond fracture as the changes of the current in a fiber after a bond failure are much more gradual.

V. BRITTLE FAILURE OF FIBER NETWORKS

Next we embark on a study of the failure characteristics of planar fiber networks in the regime where fiber failure is the dominating process. We have chosen to study this case first because it is numerically much easier than the ''bond-breakage'' one, and second because it is directly comparable to earlier random-fuse network simulations of the failure of brittle materials and composites.[10,15,16].

The conductivity stays approximately constant for $T_f=2-4$ and $N_f=5N_{f,c}$ when the system dimensions are varied. When $T_f\leqslant 1$, the conductivity is reduced slightly with increasing system size. Close to the connectivity percolation point, $N_f\approx N_{f,c}$, the conductivity decreases more rapidly, indicative of an increasing correlation length in the system. Figure 5 shows the scaling of σ_{eff} as a function of σ_s/σ_b. The results show that the effective medium theory gives quite a good prediction for $\sigma_{eff}(\sigma_s/\sigma_b)$ when α is large. The decay of σ_{eff} with decreasing σ_s/σ_b is slightly slower in the true simulation data than in the EMA results. Moreover, at the limit of well-conducting bonds σ_{eff} is larger in the former. The shape of the numerically obtained conductivity resembles results obtained for 2D random fiber networks when fiber–to–fiber bonds are included.[4] The difference to the EMA calculation of Sec. II may be partly due to the fact that the coverage or effective thickness is still rather limited (six times the percolation density).

The breaking potential V_b is roughly constant as a function of N_f, except for very rigid fibers ($T_f=0.25$) at densities close to the percolation point (Fig. 6). On approach to the percolation point, an increase in the breaking potential similar to that seen in, e.g., diluted lattice models[16] is observed. This effect is made stronger by a decrease in the effective density due to loss of connectivity in the system resulting from the increasing rigidity of the fibers as T_f is decreased. In any case, our model differs in that respect from what one would expect for a disordered brittle fuse model with a 2D/3D transition, as V_b does not seem to relate to N_f. On the experimental side, this compares with the finding that the elastic breaking strain (defined with the relation $\epsilon_{el}=\sigma_c/E$) is of the order of 1% irrespective of the basis weight of paper or bondedness of the network.[17]

Based on the three system sizes simulated ($20\times 20\times N_f$, $50\times 50\times N_f$, and $80\times 80\times N_f$), the finite size scaling of the breaking potential follows approximately the 2D extreme scaling,[16] $V_b\sim L/\sqrt{\ln L}$ for all the values of T_f with constant N_f. Since we only have three system sizes available, it is impossible to obtain the accurate form of the finite size scaling. The rupture current I_b displays saturation as a function of T_f as expected, and is a linear function of N_f, scaling as $I_b\sim L^{0.8-0.9}$ for constant N_f for all values of T_f. Alternatively, I_b can be fitted quite well with an extreme scaling-type form.[16] The small number of system sizes simulated prevents us from differentiating between the two cases.

The distribution of currents in the connections saturates if the fibers become very flexible. A less obvious result is the saturation of the high current end of the distribution also as a function of N_f, which can be perceived in Fig. 7. The simple conclusion is that this is another sign of the effective ''2D'' nature of the networks. This is because the distribution of segment stresses in a two-dimensional random fiber system saturates in the same way.[4,7] Please note that the number of

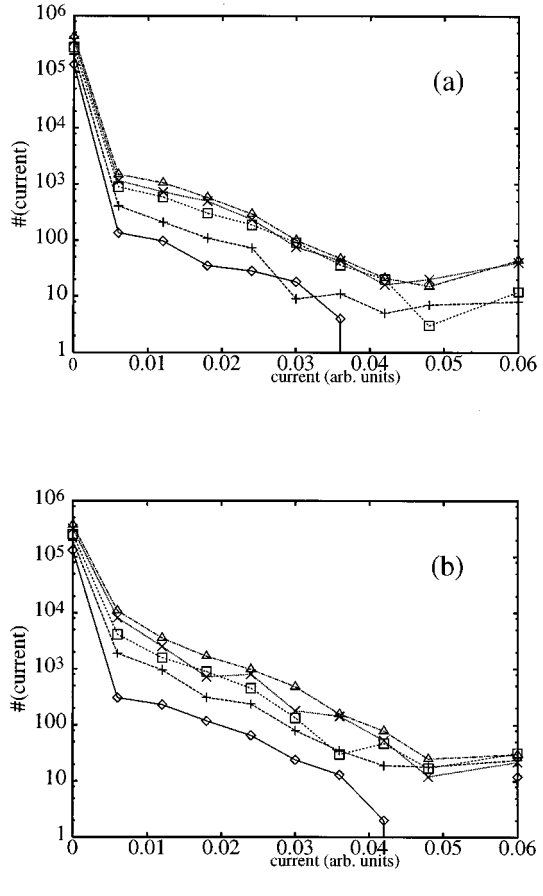

FIG. 7. Current distributions for several values of N_f. System size is $4.5l_f \times 4.5l_f$ in the xy plane, $T_f = 0.25$ (a) and 4.0 (b). ($\triangle$) $N_f = 6.25N_{f,c}$, (X) $N_f = 5N_{f,c}$, ($\square$) $N_f = 3.75N_{f,c}$, (+) $N_f = 2.5N_{f,c}$, ($\diamond$) $N_f = 1.25N_{f,c}$.

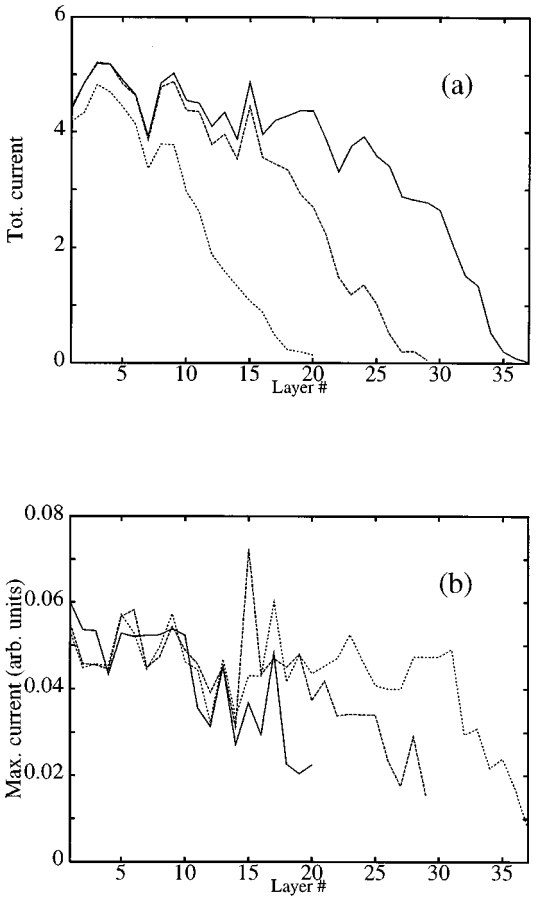

FIG. 8. Total current in all of the three lattice directions (a) and maximum current (b) as a function of the height from the substrate surface. Single simulation result. System size is $4.5l_f \times 4.5l_f$ and $T_f = 1$. (—) $N_f = 5N_{f,c}$, (– – –) $N_f = 3.8N_{f,c}$, (.....) $N_f = 2.5N_{f,c}$.

small currents does not seem to saturate equally well. Except for the small values of the currents, the curves can be quite well collapsed on top of each other by equating the integrals of the individual distributions.

We also analyzed the distributions of currents depending on the location of the bond/fiber in the network in the out-of-plane direction. This was done by plotting both the local average current and the largest current as functions of the z coordinate of the layer (Fig. 8). The total current was computed by summing the absolute values of currents in all the three principal directions in the lattice for each lattice point and the maximum current was obtained by choosing the largest of the absolute values of the three currents in the principal directions. After this was done, the currents with the same z coordinate were summed in both cases. The figures indicate that the current distribution is slightly nonuniform, but much less so for the maximum currents. The anisotropy comes from the way the networks are formed: as a three-dimensional structure is being grown, the network surface is rough,[11] which makes the actual fiber density in the top layers smaller. This naturally results in a ''smaller'' value for total current in there. In view of these results, the constancy of the current distributions seems to stem from most of the current in all layers being quite small, whereby only the low end of the current distribution is affected by the increase in the number of layers. A close inspection of the figures reveals that there is a small increase in the number of currents at the highest end of the current distribution. Large values of i are indicative of current flowing through narrow bridges between larger-than-average pores in the system.

The best guess as to why the high current end of the current distribution saturates would be that the defects or inhomogeneities that give rise to it are ''in-plane'' and thus the addition of more layers of fibers plays no role. If an increasing network thickness would give rise to truly 3D ''defect geometries'' this would be visible as changes in the distribution as well. Of course, judging such differences from our data may be difficult. The slope of the current distribution (Fig. 7) does not depend on T_f. This may seem surprising at first sight, but the explanation is quite natural. When T_f is increased (i.e., fibers are made more flexible), the average segment length is reduced. The current going through the lattice is redistributed among the shorter segments. Due to the fact that the tail of the current distribution $n(i)$ is exponential, the form of the distribution is not affected, although the tail is moved upwards. This can be seen in Fig. 7 both from the absolute scale and the relative height of the zero-current peak.

On the other hand, the system size has an effect on the slope of the tail. If the tail of the distribution is parametrized

as $n(i) \sim e^{-\beta i}$, for $L=3$, 7 and $11 \times l_f$ the decay parameters are $\beta = 166$, 200, and 400, respectively. This steepening of the distribution can be attributed to boundary effects. The high-end tail of the current distribution is always exponentially independent of T_f, which indicates that the effective medium model [Eq. (5)] presented earlier does not work for low values of T_f. Like the other breaking quantities, the total number of broken connections saturates with increasing T_f. N_b is approximately a linear function of N_f with a finite size scaling $N_b \sim L^{0.9-1.1}$ for all T_f for constant N_f. For comparison, the random breaking limit model in 2D gives $N_b \sim L$ + const for weak disorder and $N_b \sim L + L^{1.6}$ for strong one. This result is an indication of the brittle nature of fracture in the system and shows that in our simulations, networks fail by the formation of a roughly linear crack from a seed defect.

VI. DISCUSSION

We have analyzed the fracture of planar fiber networks with a simple lattice model for the electrical analogue of brittle elastic failure. The goal has been the study of the role of the geometrical inhomogeneities in the fracture processes, especially the inclusion of naturally occurring pores in such systems. The main finding is that at least in the fiber-failure controlled regime the networks become quasi- 2D regardless of the thickness. This concept together with the numerical results in general indicate that the failure of the networks is induced by ''internal defects,'' i.e., by geometry fluctuations away from the network surfaces, because on the surface the connectivity and average current are lower than in the inside of the sample.

We have also analyzed the role of the intra-fiber current transfer and the segment length distributions with an Effective Medium Approximation-type calculation. Comparisons with numerical simulation results for the conductivity agree qualitatively except perhaps for very efficient current transfer (rigid intra-layer bonds in the elastic case). In that case the EMA theory may underestimate the conductivity (resp. elastic modulus) of the system. It can also be used to analyze the qualitative dependence of the failure point on the ''stress transfer efficiency,'' and we find that the fracture voltage (corresponding to fracture strain) has a negative power law dependence on the conductivity of the bonds.

The number of broken connections, being dependent on the connectivity in the system, saturates as a function of fiber flexibility. The results indicate that the current flowing through the system consists of a ''bulk'' component and a ''tail'' part, the latter of which appears to be independent in form of the number of fibers. The bulk part grows steadily with the number of fibers in the system. This is similar to what has been seen in mechanical Finite Element Method simulations of 2D random fiber networks. These observations reinforce the main point of our paper.

The expected fracture characteristics of brittle, planar fiber networks have here been shown to comply with generic 2D models for the failure of disordered media. This includes similar size-scaling behavior for V_b and I_b, and trivial-type damage scaling as the fraction of fibers breaking versus system size. It would thus be interesting to compare by simulating the effect of i_c^z / i_c^{xy} in the region where it is smaller than unity, i.e., in the ''bond breaking'' territory. From the experimental point of view the result that the failure voltage (''stress'') does not depend on network thickness is a verifiable prediction and agrees with what is known about the failure of fiber networks in the form of paper.

ACKNOWLEDGMENTS

The authors thank the Center for Scientific Computing (CSC) in Otaniemi, Finland for generous computing resources. This work has been supported by the Technology Development Center of Finland (TEKES) and the Academy of Finland. VIR thanks Dr. Jan Åström and Dr. Per-Johan Gustafsson for useful comments.

[1] M. Murat, M. Anholt, and H. D. Wagner, J. Mater. Res. **7**, 3120 (1992).
[2] L. Monette, M. P. Anderson, and G. S. Grest, J. Appl. Phys. **75**, 1155 (1994).
[3] M. Deng and C. T. J. Dodson, *Paper—an engineered stochastic structure* (TAPPI, Atlanta, GA, 1994).
[4] V. I. Räisänen, M. J. Alava, K. J. Niskanen, and R. M. Nieminen, J. Mater. Res. (to be published).
[5] V. I. Räisänen, M. J. Alava, R. M. Nieminen, and K. J. Niskanen, Nordic Pulp Pap. Res. J. **11**, 243 (1996).
[6] S. Roux and A. Hansen, J. Physique **2**, 1007 (1992).
[7] J. Åström, S. Saarinen, K. Niskanen, and J. Kurkijärvi, J. Appl. Phys. **75**, 2383 (1994).
[8] S. Heyden, Licentiate thesis, Division for structural analysis report TVSM-3019, Lund University, Sweden, 1996.
[9] A. Jangmalm and S. Östlund, Nordic Pulp Pap. Res. J. **10**, 156 (1995).
[10] See e.g., chapters by A. Hansen, P. Duxbury, and L. de Arcangelis in *Statistical Models for the Fracture of Disordered Media,* edited by H. J. Herrmann and S. Roux (North-Holland, Amsterdam, 1990).
[11] K. J. Niskanen and M. J. Alava, Phys. Rev. Lett. **73**, 3475 (1994).
[12] E. K. O. Hellén, M. J. Alava, and K. J. Niskanen, J. Appl. Phys. **81**, 6425 (1997).
[13] P. M. Duxbury, R. A. Guyer, and J. Machta, Phys. Rev. B **51**, 6711 (1995).
[14] S. Kirkpatrick, Rev. Mod. Phys. **45**, 574 (1973).
[15] P. M. Duxbury, P. D. Beale, and C. Moukarzel, Phys. Rev. B **51**, 3476 (1995); C. Moukarzel and P. M. Duxbury, J. Appl. Phys. **76**, 4086 (1994).
[16] P. M. Duxbury, P. L. Leath, and P. D. Beale, Phys. Rev. B **36**, 367 (1987); Phys. Rev. Lett. **57**, 1053 (1986).
[17] This applies to an elongation test performed with a reasonably rapid strain rates (10%–100%/min) in the machine direction of paper so that the viscoelasticity of the fibers does not play any role.